

P-7-15

## Fiber Pump Semiconductor Lasers with Optical Antiguiding Layers for Horizontal Transverse Modes: Dependence on Mesa Width

Masafumi Fujimoto, Naoki Shomura, and Takahiro Numai

Graduate School of Science and Engineering, Ritsumeikan University  
1-1-1, Noji-Higashi, Kusatsu, Shiga 525-8577, Japan  
Phone: +81-77-561-5161 E-mail: numai@se.ritsumei.ac.jp

### 1. Introduction

High power 980-nm semiconductor lasers are used as pumping sources of erbium doped optical fiber amplifiers and contribute to wavelength division multiplexing optical fiber communication systems [1]. To reduce the number of pumping sources and to improve performance of optical fiber communication systems, higher light output power is desired for 980-nm semiconductor lasers. Generally, 980-nm semiconductor lasers have ridge structures so as not to expose their active regions to air during their fabrication processes. With an increase in injected current, kinks appear in current versus light-output ( $I$ - $L$ ) curves [2]. These kinks are associated with lasing in higher order transverse modes, which is attributed to changes in local gain profile and refractive index due to spatial hole burning, free carrier plasma effect, and heating. Slope efficiency and fiber coupling efficiency above kink levels are lower than those below kink levels. Therefore, higher kink levels are needed to achieve lasing in the fundamental transverse mode with high light output power maintaining high slope efficiency and high fiber coupling efficiency. Up to now, to increase kink levels, coupling of the optical field to the lossy metal layers outside the ridge [3], highly resistive regions in both sides of ridge stripe [4], and incorporation of a graded V-shape layer [5] have been studied. Recently, a novel ridge structure with optical antiguiding layers has been proposed by the authors [6].

In this paper, dependence of lasing characteristics of the ridge structure with optical antiguiding layers on the mesa width  $W$  is analyzed. It is found that kink levels are enhanced with a decrease in  $W$  by suppressing spatial hole burning and lowering optical gains for higher order transverse modes to the center of the active region. Also, threshold current is decreased by concentration of injected current into the active region below the mesa.

### 2. Laser Structure and Device Simulation

Figure 1 illustrates schematic cross-sectional views of (a) a conventional ridge structure and (b) the ridge structure with optical antiguiding layers for horizontal transverse modes. In Fig.1,  $\Delta t$  is a step in the guiding layer, and  $d$  is a distance from the bottom of the mesa to the bottom of the upper guiding layer. It should be noted that this step  $\Delta t$  leads to antiguiding effect. Rectangular mesa width is  $W$ , the bases are 60  $\mu\text{m}$  wide, and the cavities are 1200  $\mu\text{m}$  long. Reflectivity of the front facet and reflectivity of the rear facet are 2% and 90%, respectively. In the ridge structure shown in Fig.1 (b), due to the optical antiguiding layers with thickness of  $t_0 + \Delta t$  for horizontal transverse modes

at both sides of the mesa, optical confinement of higher order transverse modes to the center in the mesa is weakened and the modal gain of higher order transverse modes decreases. As a result, it is expected that oscillations of higher order transverse modes are suppressed even when injected current is high. In this paper, the step in the guiding layer  $\Delta t$  at both sides of the mesa is 50 nm. As shown in Fig.1 (b), undoped guiding layers below the mesa are thinner than those in side regions. Therefore, it is expected that the injected current efficiently flows into the active region below the mesa, and spreading of the injected current into the side regions is suppressed.

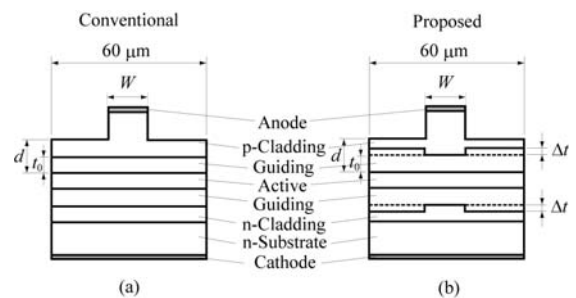


Fig.1 Schematic cross-sectional views of (a) a conventional ridge structure and (b) the ridge structure with optical antiguiding layers for horizontal transverse modes.

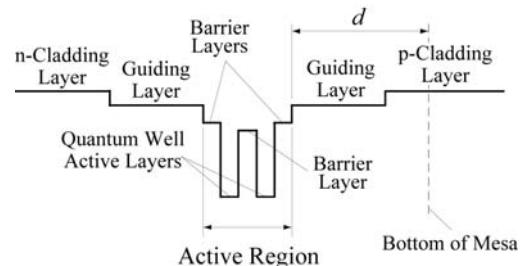


Fig.2 Energy level diagram of the conduction band in the vicinity of the active region.

Figure 2 shows an energy level diagram of the conduction band in the vicinity of the active region in Fig.1, which is the same as that in [7]. The active region has a separate-confinement heterostructure (SCH) with  $\text{Al}_{0.1}\text{Ga}_{0.9}\text{As}$  barrier layers, an  $\text{Al}_{0.03}\text{Ga}_{0.97}\text{As}$  barrier layer, and double  $\text{In}_{0.2}\text{Ga}_{0.8}\text{As}$  strained quantum well (QW) active layers. In Fig.2, the guiding layers, barrier layers, and active layers are undoped to suppress internal optical loss due to free carrier absorption. Lasing characteristics are analyzed without including any thermal effects by using a device simulation software, ATLAS (Silvaco).

### 3. Simulated Results and Discussions

Figure 3 shows electron concentration distributions in the active layers as a function of the distance from the center of the mesa in a horizontal direction for (a)  $\Delta t = 0$  nm and (b)  $\Delta t = 50$  nm when  $d=250$  nm and the injected current  $I=120$  mA, which is below the threshold current for the first order transverse mode. The parameter is the mesa width  $W$ . As shown in Fig. 3 (a) and (b), spatial hole burning is decreased with a decrease in  $W$ . Also, for  $\Delta t = 50$  nm, spatial hole burning is less significant and the electron is more concentrated in the center of the mesa than for  $\Delta t = 0$  nm. Therefore, it is expected that more stable single transverse mode oscillations and lower threshold current are obtained with a decrease in  $W$  for  $\Delta t=50$  nm than for  $\Delta t=0$  nm.

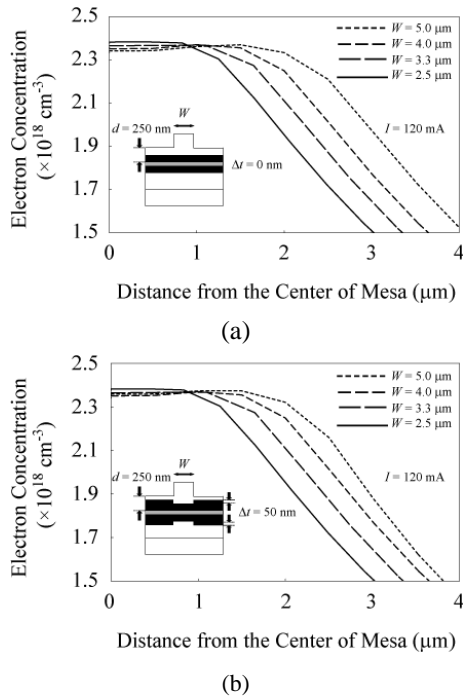


Fig.3 Electron concentration distributions in the active layers for (a)  $\Delta t = 0$  nm and (b)  $\Delta t = 50$  nm when  $d=250$  nm and the injected current  $I=120$  mA. The parameter is the mesa width  $W$ . A solid line, a long-dashed line, a dashed line, and a short-dashed line correspond to  $W = 2.5, 3.3, 4.0, 5.0$   $\mu\text{m}$ , respectively.

Figure 4 shows kink level as a function of the mesa width  $W$ . Open marks and closed marks correspond to  $d = 250$  and  $300$  nm, respectively. The kink level monotonically increases with a decrease in  $W$  and the kink level for  $\Delta t = 50$  nm is much higher than that for  $\Delta t = 0$  nm. For  $W = 2.5-5.0$   $\mu\text{m}$  with  $d = 250$  nm, the kink level increases from  $70.2$  mW to  $502$  mW when  $\Delta t = 50$  nm, while the kink level increases from  $47.5$  mW to  $216.5$  mW when  $\Delta t = 0$  nm. Especially, for  $W = 2.5$   $\mu\text{m}$  with  $d = 300$  nm, the kink does not appear when  $I$  is up to  $2$  A.

Figure 5 shows threshold current for the fundamental transverse mode  $I_{th}$  as a function of the mesa width  $W$ . Open marks and closed marks correspond to  $d = 250$  and  $300$  nm, respectively. The threshold current  $I_{th}$  mono-

tonically decreases with a decrease in  $W$  and  $I_{th}$  for  $\Delta t = 50$  nm is lower than that for  $\Delta t = 0$  nm. For  $W = 2.5-5.0$   $\mu\text{m}$  with  $d = 250$  nm,  $I_{th}$  decreases from  $59.8$  mA to  $45.8$  mA when  $\Delta t = 50$  nm, while  $I_{th}$  decreases from  $63.8$  mA to  $49.7$  mA when  $\Delta t = 0$  nm.

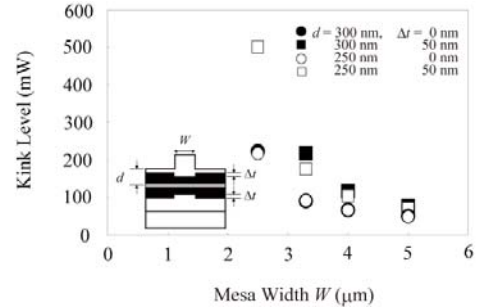


Fig.4 Kink level as a function of the mesa width  $W$ . Open marks and closed marks correspond to  $d = 250$  and  $300$  nm, respectively.

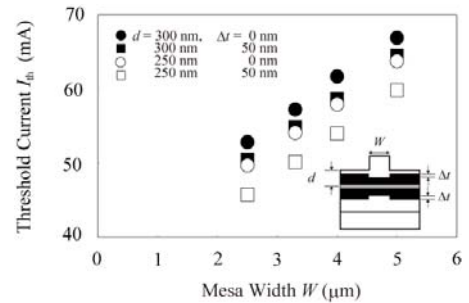


Fig.5 Threshold current for the fundamental transverse mode  $I_{th}$  as a function of the mesa width  $W$ . Open marks and closed marks correspond to  $d = 250$  and  $300$  nm, respectively.

### 4. Conclusions

In summary, dependence of lasing characteristics of the ridge structure with optical antiguiding layers on the mesa width  $W$  was analyzed. It was found that the threshold current and kink levels are improved, with a decrease in  $W$ .

### References

- [1] C. S. Harder, L. Brovelli, H. P. Meier, and A. Oosenbrug, Proc. Optical Fiber Communication Conf. '97, February, FC1, 1997.
- [2] M. F. C. Schemmann, C. J. van der Poel, B. A. H. van Bakel, H. P. M. M. Ambrosius, A. Valster, J. A. M. van den Heijkant, and G. A. Acket, Appl. Phys. Lett., vol.66, 920, 1995.
- [3] M. Buda, H. H. Tan, L. Fu, L. Josyula, and C. Jagadish, IEEE Photonics Technol. Lett., vol.15, 1686, 2003.
- [4] M. Yuda, T. Hirono, A. Kozen, and C. Amano: IEEE J. Quantum Electron., vol.40, 1203, 2004.
- [5] B. Qiu, S. D. McDougall, X. Liu, G. Bacchin, and J. H. Marsh: IEEE J. Quantum Electron., vol.41, 1124, 2005.
- [6] N. Shomura, M. Fujimoto, and T. Numai: IEEE J. Quantum Electron., vol.44, 2008, in press.
- [7] J. Temmyo and M. Sugo: Electron. Lett., vol.31, 642, 1995.